Defence Science Journal, Vol. 74, No. 1, January 2024, pp. 100-107, DOI : 10.14429/dsj.74.18981

Development and Airworthiness Certification of the Ti-6Al-4V Inlet Casing Inner Forging

P. Vignesh, Praveen K.V., Krishnakumar S., C.M. Bhuvaneswari, Shirish Sharad Kale and T. Ram Prabhu*

DRDO-Centre for Military Airworthiness and Certification, Bengaluru – 560 017, India

**E-mail: ramprabhu.t@gmail.com*

ABSTRACT

The inlet casing inner has manufactured using Ti-6Al-4V alloy through a closed die-forging route. It undergoes cyclic loads in addition to operating in extreme conditions in high-temperature environments. The demanding mission requirement of these engines necessitates the inlet casing inner to be flawless throughout its life cycle while retaining its structural integrity. It makes the qualification for airworthiness of the casing, a daunting task. In addition, the qualification tests also help to evaluate the design and manufacturing processes (closed die forging) of the inlet casing inner. The tests also provide data for further improvement of the inlet casing inner in terms of strength and fatigue life. It helps to ensure that the inlet casing inner will be able to perform as expected throughout its operational life. All the batch and consolidated test results comply with the relevant ASTM, MIL standards, and test schedule requirements.

Keywords: Inlet casing inner; Ti-6Al-4V alloy; Closed die forging; Mechanical properties; Airworthiness certification

1. INTRODUCTION

One of the important strategies for improving performance, fuel efficiency, cost-effectiveness, and reducing Green House Gas (GHG) emissions is mass reduction in the Aerospace industry[1]. It is necessary to find ways to move people and commodities that are effective, safe, inexpensive, and have little impact on the environment, whether or not they use various modes of transportation. The development of lightweight materials, such as Carbon Fibre Reinforced Polymer (CFRP), Titanium (Ti), and Aluminum (Al), used either as single, composite, or hybrid materials, has given the Aerospace industry the opportunity to reduce mass, enhance performance, and increase resource and cost efficiencies[2-3]. Ti alloys are an essential alloy in aircraft engines.

Several properties such as a high strength-to-weight ratio, excellent elevated temperature stability upto 450-600 ^{o}C, low thermal expansion, superior hot corrosion resistance, and fatigue and creep resistance make them important alloys in hot high/low-pressure compressor and turbine of the jet engine parts[4-5]. The Ti alloy content and the resultant crystal structure, the Ti-alloys are categorized into three groups; alpha (α) alloy, β (beta) alloy, and α-β (alpha-beta) alloy systems. Alpha (α) alloy typically has higher strength but lower ductility and is best suited for components that require high stiffness and strength. Beta (β) alloy has higher ductility and is suitable for components that need to withstand dynamic loads. Alpha-beta (α-β) alloy combines the properties of both alpha and beta alloys and provides the best balance between strength and ductility[6-8]. This makes α-β titanium alloys highly suitable for applications such as aerospace components, turbine blades, and other components that require a combination of high strength and resistance to environmental effects[9-10]. Different alloys have different properties, making them ideally suited for various applications. The selection of the right alloy for a specific application is important to ensure maximum performance. Ti alloys exhibit good creep strength and oxidation resistance at elevated temperatures. However, their low-temperature toughness and environmental embrittlement remain two major drawbacks. Therefore, selecting suitable heat-treatment cycle are being explored to overcome these shortcomings[11].

To achieve better properties and structural integrity under critical operating conditions, all rotating components must be forged to meet airworthiness certification requirements. It is more cost-effective to forge inlet casing inner made of Ti-6Al-4V alloy in order to obtain symmetric properties across the contour of the forging[12]. The main purpose of the forging process is to achieve the desired shape and properties that can't be obtained from a bar or billet[13]. Forging is primarily used to obtain a desired shape and property that is not possible in bars or billets. Forging processes alter the microstructure of Ti-6Al-4V differently because it is strain-sensitive. Typically, these forgings are made from closed-die forging routes in order to have improved properties and microstructure consistency[14]. The α-β condition is suitable for the forging of Ti-6Al-4V because it provides better mechanical properties than the α and β only conditions. The desired microstructure and mechanical properties can be achieved by controlling the cooling rate and the β transit temperature[15].

To understand how processing parameters affect microstructure and mechanical properties in the high-

Received : 20 April 2023, Revised : 23 June 2023
Accepted : 25 August 2023, Online published : 12 January 2024

temperature deformation of Ti-6Al-4V alloy, the effects of the processing parameters were evaluated using tensile tests, creep tests, fatigue tests, and fracture toughness tests conducted at room and hot temperatures to provide the technological basis for optimizing processing parameters. The qualification tests included static and fatigue tests to evaluate the material properties, temperature response, and structural integrity of the turbine disk. The results of the tests were then used to validate the design of the turbine disk and its qualification for actual use in aero engines.

2. FORGING PROCESS DESIGN

The forging method began with the evaluation of the final component drawing. Based on the flash and root features, material forge ability, and the type of forging equipment, the stages of performing operations evolved. The billet was cut to the size of 180 mm (diameter) x 274 mm (height) by electric discharge machining. The billet was heated to 700 °C±10 °C for 1 hr in an electric resistance furnace. The dies used for the inlet casing inner forging were the Ni-Cr-Mo tool steel. The dies were finished to 0.8 µm and coated with water-based colloidal graphite lubricants. The dies were internally heated to 200 °C to minimize the die chilling effects. The inlet casing inner forging design for the present configuration had mainly three stages: (1) billet cutting, (2) upsetting, and (3) die forging. The stages of inlet casing inner closed die forging are shown in Fig. 1.

The forging temperature and soaking time are selected such that during the forging operation, the material should not crack due to die chilling and no overheating to avoid transformation of microstructure to completely beta grain structure. The billet was heated to 700 °C±10 °C for 1 hr. The molding and finishing die close operation was performed in the 3000T HP/4000T HP to form the casing. Due to the large contact area of the mold and finisher dies cavity, there is a possibility for severe heat loss of the casing by the die chilling effects that generate a steep temperature gradient in the casing during cooling. The flash was removed by trimming operation. The casing was cleaned and machined in Lathe/CNC machines to the drawing. The corner radius, fillet radius, and draft angle used in the forging process were 3R, 2R, and 5° max respectively.

Step 1: Stock Preparation, Cross Section x Length, Cutting Machine, And Horizontal Band Saw
Step 2: Face Turn and Corner Radius to R10, Lathe
Step 3: Pre-heat to 700°C±10°C for 1 Hr (min.), Heat to (Beta Transus -30°) ±10°C, Soak for 2 Hr 15 Mts (min.) – 3 Hr 30 Mts (max.), Upset to given dimensions, Cool in air, No. of heat -1, Plant: 3000T HP/4000T HP
Step 4: Pre-heat to 700°C±10°C for 1 Hr (min.), Heat to (Beta Transus -30°) ±10°C, Soak for 2 Hr (min.) – 3 (max.), Die Forge to given dimensions, Cool in air, No. of heat -2, Plant: 16T Hammer
Step 5: Drill a hole of Ø 75±5 at the center, Plant: Lathe or Drilling Machine
Step 6: Rough Machining, Plant: Lathe / CNC

3. EXPERIMENTAL PROCEDURE

3.1 Heat Treatment and Testing

The polished casings were given the following heat treatment according to the GTM-Ti-64DM/FORG specification: Solution treatment at 950-975 °C±10 °C for 1-2 hrs and followed by water quenching in agitated water and Annealing at 700±5 °C for 1-2 hrs and followed by air-cooling. The chemical composition of the casing was analysed by the atomic absorption spectroscopy (A) shown in Table 1. As part of the

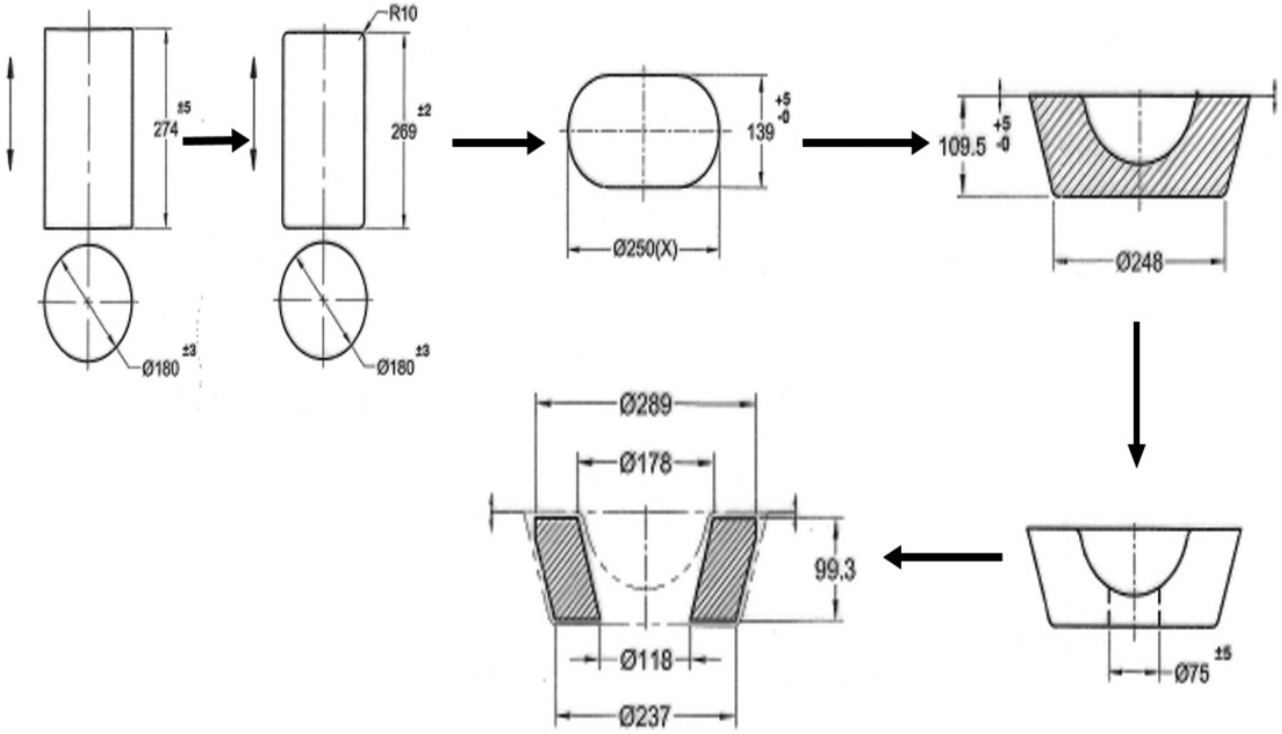

Figure 1. Closed die forging method for the Ti-6Al-4V inlet casing inner.

Table 1. In terms of its chemical composition, Ti-6Al-4V is composed of

Elements	Specification requirements	Results
Al	6.20-6.75	6.48
V	3.50-4.50	3.79
Fe	0.30 max	0.05
C	0.08 max	0.01
Y	50 (ppm) max	7.00
B	10 (ppm) max	1.0
Sn	0.10 max	0.01
Mo	0.10 max	0.01
Cu	0.10 max	0.01
Mn	0.10 max	0.01
Zr	0.10 max	0.01
Other	0.20 max	-
Ti	Bal.	Bal.

gas analysis, inert gas fusion was used to determine the gas composition per ASTM E1447 & ASTM E 1409. The casing was sectioned along the parting line and etched to reveal the grain flow pattern. The samples from the casing were prepared to 1 µm polish for the microstructure examination. The Krolls reagent was used as an etchant to reveal phases in the Ti alloy.

The microstructure examination and grain flow examination procedures followed the ASTM E3/E407 and ASTM E340 standards, respectively. The procedure for microstructure examination and grain flow examination was as per the ASTM E3/E407 and ASTM E340 standards respectively. The samples extracted from the casing were tested for room tensile (ASTM E8), notch tensile (ASTM E602) and high temperature tensile (ASTM E21). Following ASTM E399, fracture toughness (K_1C) is measured. Low cycle fatigue tests were performed on specimens under rotating bending loading (stress ratio R = 1) with a frequency of 1.5 Hz per ASTM E606.

The creep tests were conducted on axial tensile creep test machines as per ASTM E139. As part of the preparation for the test, the sample was heated in a high-temperature furnace for 1 hr at 300 °C before being placed in the furnace for testing. The inlet casing inner was inspected non-destructively using Ultrasonic as per AMS 2631 and fluorescent penetrant examination (FPE) to the Mil-Std 1907 standard Grade C acceptance criteria. The penetrant used was of the dry developer, the sensitivity level of II, and rough machined surface condition was selected for FPE examination.

4. RESULTS AND DISCUSSION

4.1 Chemical Analysis and Gas Analysis of Ti-6Al-4V

The chemistry meets GTM-Ti-64 DM/ FORG (REV-5) requirement. The high affinity of Ti for hydrogen, oxygen, and nitrogen makes it necessary for the heat treatment to be carefully controlled to avoid excessive contamination of the material. H_2 in particular was monitored to check for hydrogen embrittlement, which is produced by the creation of hydrides. To avoid hydrogen embrittlement, the alloy is expected to have H_2 less than 100 ppm as shown in Table 2. The alloy with an alpha + beta structure can tolerate high hydrogen content than all the alpha alloys before embrittlement becomes noticeable due to the higher solubility of hydrogen in the beta phase. The oxygen has a high affinity to Ti. The diffusion of oxygen stabilizes the α-phase, which leads to a decrease in ductility[16].

Table 2. Gas analysis in Ti-6Al-4V

Elements	Specification requirements	Results
Hydrogen	100 (ppm)	48 (ppm)
Nitrogen	0.03 (wt %)	0.0005 (wt %)
Oxygen	0.16-0.2	0.174 (wt %)

4.1 Microstructure and Grain Flow Pattern

The microstructure consists of nearly equiaxed alpha (α) grains in the transformed beta (β) matrix, as seen in Fig. 2. Equiaxed structure is important for the highest strength/ductility combination and fatigue strength. The equiaxed duplex structure is preferred for the casing forging. There is no evidence of low-density inclusions such as hard α, β flecks, or cavities in the microstructure implying the sound quality of the forging. The grain flow lines clearly follow contour shapes, as seen in Fig. 3. Macro examination of the sample revealed a satisfactory uniform macrostructure, free from laps, folds, segregation, voids, inclusions, dirt, and dross & other abnormalities. This confirms the uniform metal flow during the forging process.

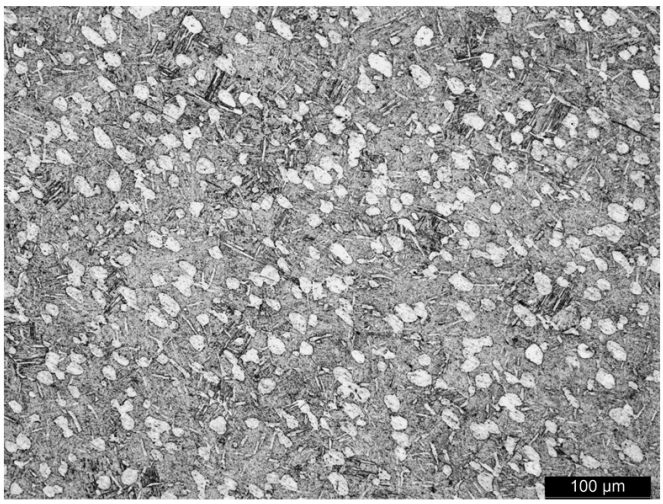

Figure 2. Microstructure of the Ti-6Al-4V inlet casing inner.

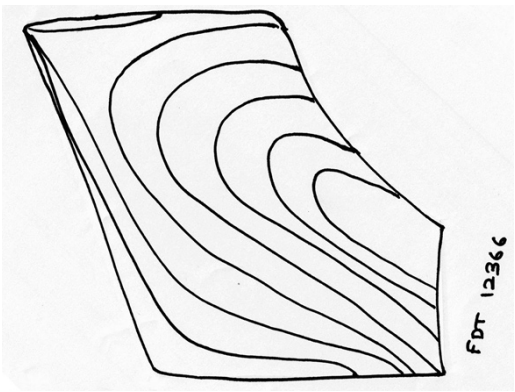

Figure 3. Cut section grain flow pattern.

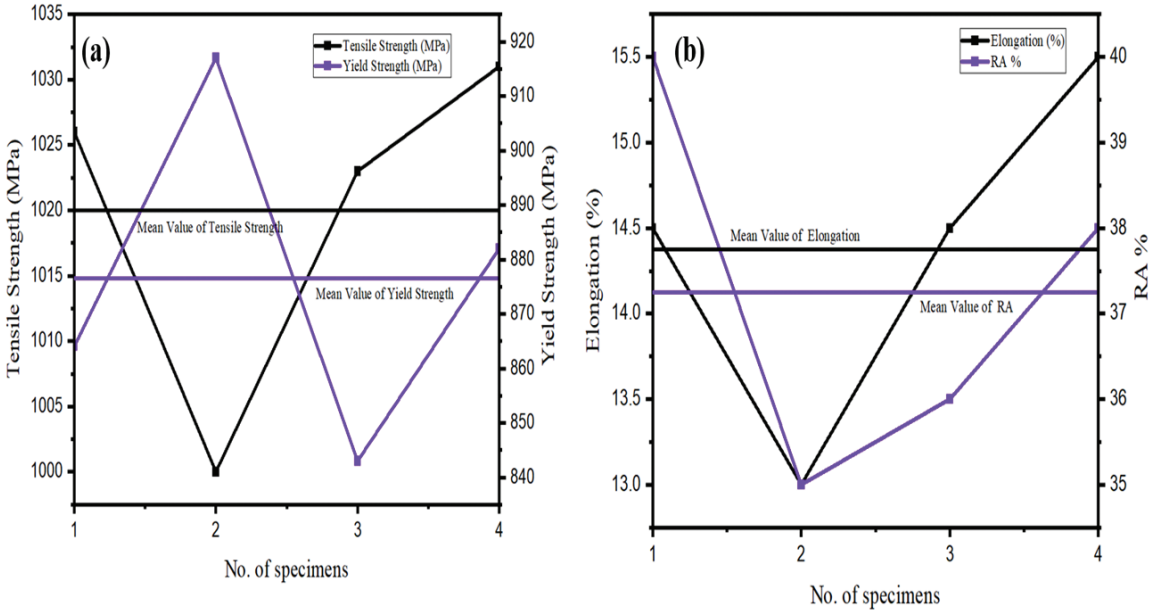

Figure 4. Mechanical properties of Ti-6Al-4V in solution treated and annealed condition.

The equiaxed area free of distortion indicates that the metal moved during the forging operation after the forging stock was heated in the range of β. This structure is known as a duplex structure, which consists of a mixture of α and β grains. The final microstructure is dependent on the composition of the alloy, as well as the cooling rate[17]. From Fig. 3 it can conclude that proper control of metal flow was required in the forging of Ti-6Al-4V in order to ensure acceptable mechanical characteristics.

4.2 Mechanical Properties

Average values from tensile properties were obtained from specimens of 4 different heats, tested at room temperature, notched tensile, and 300 °C in solutionized and annealed conditions. Figure 4 summarises the results of four different uniaxial tensile tests. Since the microstructural morphology did not change, it is obvious that the differences are not very prominent. Hall[18] and Petch[19] have argued that dislocation pile-up is caused by grain or phase boundaries during plastic deformation, resulting in a pile-up of dislocations. In accordance with the Hall-Petch relation, a finer microstructure can result in higher strength[20]. It has also been suggested that the remaining elastic and plastic strains from the forging process may strengthen the material, and this density of dislocations in the un-recrystallized grains is suspected to be an important contributing factor to it.

The mechanical properties increase at the expense of ductility with the inclusion of a notch. The notch tensile test is shown in Table 3. A ratio of 1.54 is observed between notch tensile strength and smooth tensile strength. This value indicates that the alloy is notch sensitive. The high temperature (300 °C) tensile properties are shown in Table 4. When the alloy is subjected to elevated temperature, it loses its strength by various mechanisms such as activation of pyramidal and prismatic slip system, dislocation creep (climb, cross slip), wedge intergranular cracking, grain coarsening, and α to β transformation[21]. The increase in ductility is indicative

Table 3. Notch tensile testing in solution treated and annealed condition

Condition	UTS (MPa)	Ratio of Notched tensile strength to smooth tensile strength (Specified 1.3 or more)
Room temperature	1384	1.34
	1544	1.54
	1533	1.49
	1759	1.70
Average	1555	1.51

Table 4. High temperature tensile properties

Condition	0.2 % PS (MPa)	Tensile strength (MPa)	% Elongation	RA %
300 °C	604	719	15	40
	581	679	19.5	46
	630	734	17.5	44
	649	750	15	42
Average	616	721	16.75	43

of the activation of pyramidal and prismatic slip systems and more α to β transformation. As the β-phase is a BCC structure and comparatively more ductile than the α-phase (HCP), the deformation is easier with the increase of β phase fraction. Further, the activation of the slip system facilitates the deformation resulting in improved ductility at the expense of strength[22]. It is possible to estimate fracture toughness by observing the failure of specimens due to fatigue cracks. This balance (strength/ductility/fracture toughness) is in satisfactory agreement with the results of plane strain fracture toughness tests performed in accordance with ASTM E399 for the Ti-6Al-4V alloy that was forged in solutionized and annealed

conditions. KIC for Ti-6Al-4V varies greatly depending on the operational procedure and crack extension, and it is difficult to measure it with less than one-inch thickness under ASTM E399. Rather than a plane stress to plane strain transition, Ti-6Al-4V exhibits high ductility and R-curve, along with a 2 per cent crack extension The longer the crack extension, the more likely it is that thick specimens will show higher values of measured fracture toughness than thin specimens do. This is because the longer crack extension is driving the result higher on the R-curve than the shorter extension[23].

The specimens were then tested at room temperature and the results indicated that the forging was able to withstand the conditions. The results showed that the forging was of excellent quality, with a fracture toughness value (58 ksi√in.) well above the minimum required for the application. The fatigue properties of the inlet casing inner are summarized in Table 5. The microstructure still plays an important role in determining the fatigue strength. The fatigue life can be further improved by optimizing the microstructure. Therefore, the microstructure should be carefully considered when designing components for fatigue. The effective crack growth (ECG) paths are the most critical in the fracture process. They have the highest growth rate and thus the greatest potential to cause fracture failure.

Table 5. Low cycle fatigue properties of the Ti-6Al-4V inlet casing inner

Specimen condition	Stress (MPa)	Frequency (Hz)	Minimum life cycle
Room temperature	41.5-830	1.5	10200
			10300
			10300
			10400

The understanding and prediction of these paths are essential to optimise the design of materials and components. The dimples will then occur once the effective cracks meet[24]. The fracture toughness can be determined through experiments and can be used to predict the fracture and fatigue properties of a material. This information is essential in designing components to withstand mechanical loads in various applications[25]. Microstructural features such as grain boundaries, sub-grain boundaries, grain orientation, residual stresses, and dislocation structures play an important role in crack behavior, as long as a crack is microstructurally short[26]. Because of solutionizing and annealing, the microstructure is free of residual stress and dislocation density, as well as having no sub-grain boundaries. The Hall-Petch equation also holds true for fatigue strength and is well-matched to tensile behavior in explaining fatigue strength.

In Table 6, the creep characteristics, for each sample are shown. Usually, creep behavior is reflected by a steady-state creep rate and residual deformation, which are used to predict creep behavior. The load is transferred from the α and β phases, and the stress within each phase changes. This change in stress causes a redistribution of load within each phase, resulting in the load being shared among the individual particles within each phase. Highly loaded phases break at the points where the stresses are highest and where flaws accumulate as they

Table 6. Creep properties of the Ti-6Al-4V inlet casing inner

Sample condition	Stress (MPa)	Duration (hrs)	% Plastic Strain
300 °C	500	100	0.068
			0.073
			0.077
			0.022

accumulate under high loads. During the creep deformation, the load is transferred to these locations from the surrounding phases, as a result of which further creep deformation is maintained. Additionally, the phases should impede dislocation motion within the continuous microstructure, resulting in greater creep resistance. A significant role was expected to be played by the microstructure, particularly the α -phase alone, which constitutes up to 80 per cent of the microstructure. There is an increase in phase deformation associated with elevated temperatures due to 'a' slip and some 'c+a' slip, with 'a' slip dominating for alloy microstructures. For Ti-6Al-4V alloys, the basal plane intersects the tensile axis, preventing 'a slip[20]. In this case, it is believed that creep deformation, caused by dislocation climb, is only possible for 'c+a' slip when the dislocations are interacting, which may also be another reason for the alloy's lower creep rates and higher creep resistance[27].

During tensile-creep deformation, the sequence of deformation was similar to that previously observed during experiments completed at room temperature and elevated temperatures. With increased creep strain and time, these cracks rapidly grew into macro cracks that multiplied with the increase in creep strain. The localised slip appears to have been initiated after the phase's cracking became quite extensive in the microstructure. Deformation persisted via high plasticity in the microstructure, void, and coalescence formation, and crack and coalescence creation in the phases, and finally final ductile fracture. As was the case with Ti-6Al-4V alloys, cracking was notably noticeable at the α+β surfaces[7]. Generally, Creep damage is characterized by cavities forming at grain boundaries[4]. The majority of creep life is determined by a steady creep rate that is dependent on temperature and stress. Cavities grow and increase in size and quantity when temperature and tension decrease. An Arrhenius law for temperature dependency and a power law for stress dependency is often used to describe Eqn. (1).

$$\in = A\sigma^{n} \exp(Q/RT) \quad (1)$$

The stress exponent (n) and activation energy (Q) can also be used to predict and analytically estimate the creep behavior of materials under different loading conditions. This can be used to design components that can withstand long-term deformations without failure. This paper presents results on creep at high temperatures for Ti-6Al-4V alloys that can be compared with those obtained on similar or different Ti alloys. The lowest values, n ≈ 1, have been reported for lower stress levels associated with the Harper-Dorn creep regime[5]. A new review on Ti alloy potential[9] has been published. As Banerjee and Williams suggest, these results may be supported

by threshold stress, which may result in the greatest exponent values being reduced to around 4-5[10].

4.3 Non-Destructive Testing

The raw material blank was inspected to 0.8 mm FBH defect tolerance level. The defect may be cracks, stringers, inclusion, and any other discontinuities. The engine designer decided on the defect tolerance levels.

The designer takes into consideration of static, dynamic loading state, flight envelope, temperature, safety factor, and environmental condition of the inlet casing inner and uses the standard fracture mechanics to decide the allowable defect size. For the present case, the inlet casing inner can have a single defect size of a max of 0.8 mm for the designed engine life of 1000 hr. The coupons that qualified for the Table 5 requirements were only used for making the casings. It is important to note that surface defects are usually not permitted except for inclusions in fatigue-loaded applications, as the surface is very sensitive to fatigue cracking. The casings fabricated to the forging method are given in Fig. 1. These casing forgings were inspected for surface defects using fluorescent penetrant inspection to the acceptance criteria given in Table 6. It is worth noting that the surface is free from inclusion, stringers, cracks, seams, laps, undercut, flakes, and laminations. The above two non-destructive tests are highly important from in airworthiness perspective. Without passing these two tests, the inlet casing inner is not allowed to be used in the engine.

4.4 Airworthiness Certification

The certification encompasses the process and product validation against the test schedule. Tests required to qualify the casings are decided based on the material specification and the part's working condition. The complex shape of the casings demands tensile properties evaluation in the notch condition. The safe life design of the engine makes the strict defect level tolerance of 1.2 mm FBH. Hence, in order to qualify the process and product, the following tests are mandatory: (1) mechanical testing like tensile test (smooth, notch, and hot) condition, creep test, low cycle fatigue, and fracture toughness (2) ultrasonic and fluorescent penetrant test to validate the casing defect level in a tolerable limit, (3) chemical composition to conform to the material specification and in particular, the gaseous elements level so that hydrogen embrittlement (4) grain flow pattern to validate the forging process, (5) microstructure to validate the heat treatment process. The above tests are carried out and the test reports are verified for compliance with the forging test schedule. Based on satisfactory compliance, the casing is provisionally certified for component level, engine bed testing, and flight tests. Successful qualification from the above tests, the inlet casing inner is recently certified by the Indian military airworthiness certification body (CEMILAC)[28].

Table 7. Ultrasonic examination results of the inlet casing inner

Quality class	Single discontinuity (FBH Size)	Loss of back reflection % max	Observation
AA	1.2	50	No defect is observed

5. CONCLUSIONS

The Ti-6Al-4V inlet casing inner is manufactured through the closed die forging technique. This technique involves six important stages: (1) Stock preparation, (2) Face turning, (3) Upsetting, (4) Die forging, (5) Drilling a hole, and (6) CNC/ Lathe Finishing. The microstructure of the casings shows an equiaxed α phase in a duplex α + β matrix with no evidence of low-density inclusions such as hard α, β flecks, cavities, and any other undesirable intermetallics. The casing is subjected to tensile, fatigue, creep, and impact, and the properties meet the minimum requirements of GTM-Ti-64DM/FORG. The forged casings were qualified for 1.2 mm FBH internal defect (AMS 2631) and MIL-STD 1907 Grade B surface defect requirements. Based on the above satisfactory test results, the airworthiness is ensured for the inlet casing inner.

REFERENCES

1. Hertwich, E.G.; Ali, S.; Ciacci, L.; Fishman, T.; Heeren, N.; Masanet, E.; Asghari, F.N.; Olivetti, E.; Pauliuk, S.; Tu, Q. & Wolfram, P. Material efficiency strategies to reducing greenhouse gas emissions associated with buildings, vehicles, and electronics-A review. *Environ. Res. Lett*., 2019, **14** (4). doi :10.1088/1748-9326/ab0fe3.
2. Siengchin, S. A review on lightweight materials for Defence applications: A present and future developments. *Def. Technol*., 2023, **24**, 1-17. doi: 10.1016/j.dt.2023.02.025.

Table 8. Fluorescent penetrant examination results of the inlet casing inner

Maximum Allowable discontinuity size and distribution in (mm) for fluorescent penetrant Inspection		Observations
Discontinuity	Grade B	
Inclusions**,** rounded	1.6 mm, DD-3	Nil
Inclusions**,** stringers	19 mm, DD-1	Nil
Un-machined surfaces	37.5 mm, DD-1	Nil
Seams or laps (machined surfaces)	6.35 mm, DD-1	Nil
Propagating discontinuities (Crack, flakes & laminations etc)	0	Nil
DD (Distribution Designation) Signifies the following: DD-1 Discontinuities no closer to each other than 12.5 mm Linearly and 6.35 mm in a parallel direction, DD-2 no more than two indications, DD-3 Discontinuities no closer to each other than three times the maximum size		

3. Fang, X..; Liu, L.; Lu, J. & Gao, Y. Optimization of forging process parameters and prediction model of residual stress of Ti-6Al-4V alloy. *Adv. Mater. Sci. Eng.,* 2021. doi:10.1155/2021/3105470.
4. Chen, W. The elevated-temperature creep behavior of boron-modified Ti-6Al-4V alloys. *Mater. Trans*., 2009, **50**(7), 1690-1703. doi:10.2320/matertrans.MF200914.
5. Badea, L.; Surand, M.; Ruau, J. & Viguier, B. Creep behavior of Ti-6Al-4V from 450 °C to 600 °C. *UPB Sci. Bull., Series B*, 2014, **76**(1), 185-196.
6. Gupta, A.; Khatirkar, R.K..; Kumar, A. & Parihar, M.S. Investigations on the effect of heating temperature and cooling rate on evolution of microstructure in an α+ β titanium alloy. *J. Mater. Res.*, 2018, **33**(8), 946-957. doi:10.1557/jmr.2018.54.
7. Mahadule, D.; Khatirkar, R.K..; Gupta, S.K..; Gupta, A & Dandekar, T.R. Microstructure evolution and corrosion behaviour of a high Mo containing α+ β titanium alloy for biomedical applications. *J. Alloys Compd.*, 2022, **912**, 165240. doi:10.1016/j.jallcom.2022.165240.
8. Chen, W.; Lin, Y.C.; Zhang, X. & Zhou, K. Balancing strength and ductility by controllable heat-treatment twinning in a near β-Ti alloy. *J. Mater. Res. Technol*. 2020, **9**(3), 6962-6968. doi:10.1016/j.jmrt.2020.04.045.
9. Williams, J.C. & Boyer, R.R. Opportunities and issues in the application of titanium alloys for aerospace components. *Met.,* 2020, **10**(6), 705. doi:10.3390/met10060705.
10. Singh, P.; Pungotra, H. & Kalsi, N.S. On the characteristics of titanium alloys for the aircraft applications. *Mater Today*.; 2017, **4**(8), 8971-8982. doi:10.1016/j.matpr.2017.07.249.
11. Ogunmefun, O.A.; Bayode, B.L.; Jamiru, T. & Olubambi, P.A. A critical review of dispersion strengthened titanium alloy fabricated through spark plasma sintering techniques. *J. Alloys Compd.*, 2023. doi:10.1016/j.jallcom.2023.170407.
12. Astarita, A.; Ducato, A.; Fratini, L.; Paradiso, V.; Scherillo, F.; Squillace, A.; Testani, C. & Velotti, C. Beta forging of Ti-6Al-4V: Microstructure evolution and mechanical properties. *In Key Eng*., 2013, **554**, 359-371. doi:10.4028/www.scientific.net/KEM.554-557.359.
13. Pitchugin, I.I. & Kovalev, I.A. Develop titanium-alloy blades for large steam turbines. United States: N. p., 1994. https://www.osti.gov/biblio/7101920 (Accessed on)
14. Gupta, R.K.; Kumar, V.A. & Kumar, P.R. Effect of variants of thermo mechanical working and annealing treatment on titanium alloy Ti6Al4V closed die forgings. *J. Mater. Eng. Perform*., 2016, **25**(6), 2551-2562. doi:/10.1007/s11665-016-2110-8.
15. Sieniawski, J.; Ziaja, W.; Kubiak, K. & Motyka, M. Titanium alloys: Advances in properties control. *In* Microstructure and mechanical properties of high strength two-phase titanium alloys. Titanium alloys-advances in properties control, IntechOpen London, UK, 2013, pp.69-80. doi:10.5772/56197.
16. Shaaban, A.; Nakashima, H.; Ueda, M. & Takeyama, M. Effects of oxygen addition on the microstructure, phase transformations, and oxidation resistance of TiAl alloys. *J. Alloys Compd.,* 2022, **918**, 165716. doi:10.1016/j.jallcom.2022.165716.
17. Kolli, R.P. & Devaraj, A. A review of metastable beta titanium alloys. *Metals.*, 2018, **8**(7), 506. doi:10.3390/met8070506.
18. Hall, E.O. The deformation and ageing of mild steel: II characteristics of the Lüders deformation. *Proc. Phys. Soc. Section B*, 1951, **64**(9). doi:10.1088/0370-1301/64/9/302.
19. PETCH, N. The cleavage strength of polycrystals. *J. Iron Steel Res*., 195, **174**, 25-28.
20. Wang, C.; Yu, D.; Niu, Z.; Zhou, W.; Chen, G.; Li, Z. & Fu, X. The role of pyramidal< c+ a> dislocations in the grain refinement mechanism in Ti-6Al-4V alloy processed by severe plastic deformation. *Acta Mater.*, 2020, **200**, 101-115. doi:10.1016/j.actamat.2020.08.076.
21. Fang, X.; Liu, Y.; Shao, Y.; Xu, H. & Yang, F. Forging temperature effects on crack tip creep behaviour of hot hammer forged Ti-6Al-4V alloy. *Adv. Mater. Sci. Eng.*, 2023. doi:10.1155/2023/4414502.
22. Cepeda-Jimenez, C.M.; Carreño, F.; Ruano, O.A.; Sarkeeva, A.A.; Kruglov, A.A. & Lutfullin, R.Y. Influence of interfacial defects on the impact toughness of solid state diffusion bonded Ti–6 Al–4 V alloy based multilayer composites. *Mater. Sci. Eng. A.*, 2013, **563**, 28-35. doi: 10.1016/j.msea.2012.11.052.
23. Salem, J.A.; Lerch, B.; Thesken, J.C.; Sutter, J. & Russell, R. Strength, fatigue, and fracture toughness of Ti-6Al-4V liner from a composite over-wrapped pressure vessel (No. NASA/TM-2008-215147) 2008.
24. Evans, W.J. & Harrison, G.F. Power law steady state creep in α/β titanium alloys. *J. Mater. Sci*., 1983, **18**(11), 3449-3455. doi:10.1007/BF00544173.
25. Zhou, J.Z.; Meng, X. K.; Huang, S.; Sheng, J.; Lu, J.Z.; Yang, Z.R. & Su, C. Effects of warm laser peening at elevated temperature on the low-cycle fatigue behavior of Ti6Al4V alloy. *Mater. Sci. Eng. A*., 2015, **643**, 86-95 doi:10.1016/j.msea.2015.07.017.
26. Kumar, D.; Idapalapati, S.; Wang, W. & Bhowmik, A. Microstructural characteristics and strengthening mechanisms in a polycrystalline Ni-based superalloy under deep cold rolling. *Mater. Sci. Eng. A*., 2019, **753**, 285-299. doi:10.1016/j.msea.2019.03.005.
27. Zhang, Y.; Li, D.; Li, X.; Liu, X.; Zhao, S. & Li, Y. Creep deformation and strength evolution mechanisms of a Ti-6Al-4V alloy during stress relaxation at elevated temperatures from elastic to plastic loading. *J. Mater. Sci.*

Technol., 2022, **126**, 93-105.
doi:0.1016/j.jmst.2022.02.042.
28. DDPMAS, "Framework and procedure for design, development and production of military air systems and airborne stores", 2021.

CONTRIBUTORS

Dr P. Vignesh is a Junior Specialist-1 working on the Airworthiness Certification of Casting at RCMA (F&F), DRDO-CEMILAC. His areas of interest include: Mg & Al-Casting, additive manufacturing, and materials processing for property enhancement.
Contribution in the current study: Conceptualisation, formal analysis, validation, writing, review and editing.

Mr Praveen K.V. is a Technical Staff working on the Airworthiness Certification of Forgings at RCMA (F&F), DRDO-CEMILAC. His areas of interest include: Forgings, additive manufacturing materials, and associated testing.
His current contribution in this paper is Formal analysis, validation, data curation, writing - Original Draft

Krishna Kumar S. is a Technical Staff working on the Airworthiness Certification of Forgings at RCMA (F&F), CEMILAC, DRDO. His current field is Simulation on castings & forgings, powder metallurgy. His current contribution in this paper is Validation, data curation, formatting, writing.

Mrs C.M. Bhuvaneswari is the Regional Director (F&F) working on the Airworthiness Certification of Non-Metallic Materials at RCMA (F&F), DRDO-CEMILAC. She obtained her Bachelor's degree in Chemical Engineering from NIT Trichy. Her areas of interest include: Polymers, rubbers, coatings, paints, and seals.
Her current contribution in this paper is conceptualisation, methodology, visualisation, resource management and supervision.

Dr Shirish Sharad Kale is the Director (Materials & Public Interface) working on the Airworthiness Certification of Metallic/ Non-Metallic Materials at DRDO-CEMILAC. He obtained his PhD in Metallurgical and Materials Engineering from IIT, Bombay.
His current contribution in this paper is Project administration, conceptualisation and methodology.

Dr T. Ram Prabhu is a Scientist "E" working on the Airworthiness Certification of Metallic Materials at RCMA (F&F), DRDO-CEMILAC. He obtained his PhD in Metallurgical and Materials Engineering from IIT, Madras. His areas of interest include: Additive manufacturing, material property correlations and electrochemical behaviour.
His current contribution in this paper is conceptualisation, methodology, validation, formal analysis, resource management and supervision.